Supplementary Material

Electronic Structure, Magnetoresistance and Spin Filtering in Gr|2ML-CrI$_3$|Gr van der Waals Magnetic Tunnel Junctions

Yibin Zhang,[a]   Jie Liu,[a,†] Xuan Shi,[b,c] Renhao Deng,[a] Huan Tang,[a] Hong Chen,[a] and Hongkuan Yuan,[a,†*]

[a] School of Physical Science and Technology, Southwest University, Chongqing, 400715, China
[b] School of Mechanical Engineering, Shaanxi University of Technology, Shaanxi, 723001, China
[c] Shaanxi Key Laboratory of Industrial Automation, Shaanxi University of Technology, Shaanxi,   723001, China
)   Equal contribution
*) Corresponding Author: yhk10@swu.edu.cn (Hongkuan Yuan),   Tel.: +86-023-68252355

Contents:
FIG. S1 The spin-polarized band structure and the density of state (DOS) of the monolayer CrI$_3$ obtained with PBE+U calculations. The blue and red curves denote the spin-up and spin-down bands (left panel), respectively;   blue and green lines denote the Cr and I atoms (right panel), respectively.

FIG. S2 The band structure of the graphene monolayer obtained with PBE+U calculations.

FIG. S3. (a) Spin-up density difference and (b) spin-down density difference ρ=ρ$_{(Heter)}$-ρ$_{(CrI3)}$-ρ$_{(Gr)}$ of Gr|2ML-CrI$_3$|Gr heterostructure from side-view (Isosurface value: 0.0015 e/Å^3) . Green and blue colors denote the accumulation and depletion of density regions, respectively.

FIG. S4. Band structures of Gr|2ML-CrI$_3$(AB')|Gr heterostructure with inter-layer ferromagetic (FM) ordering between CrI$_3$ layers.

FIG. S5. Band structures of Gr|2ML-CrI$_3$(AB')|Gr heterostructure with inter-layer antiferromagetic (AFM) ordering between CrI$_3$ layers.
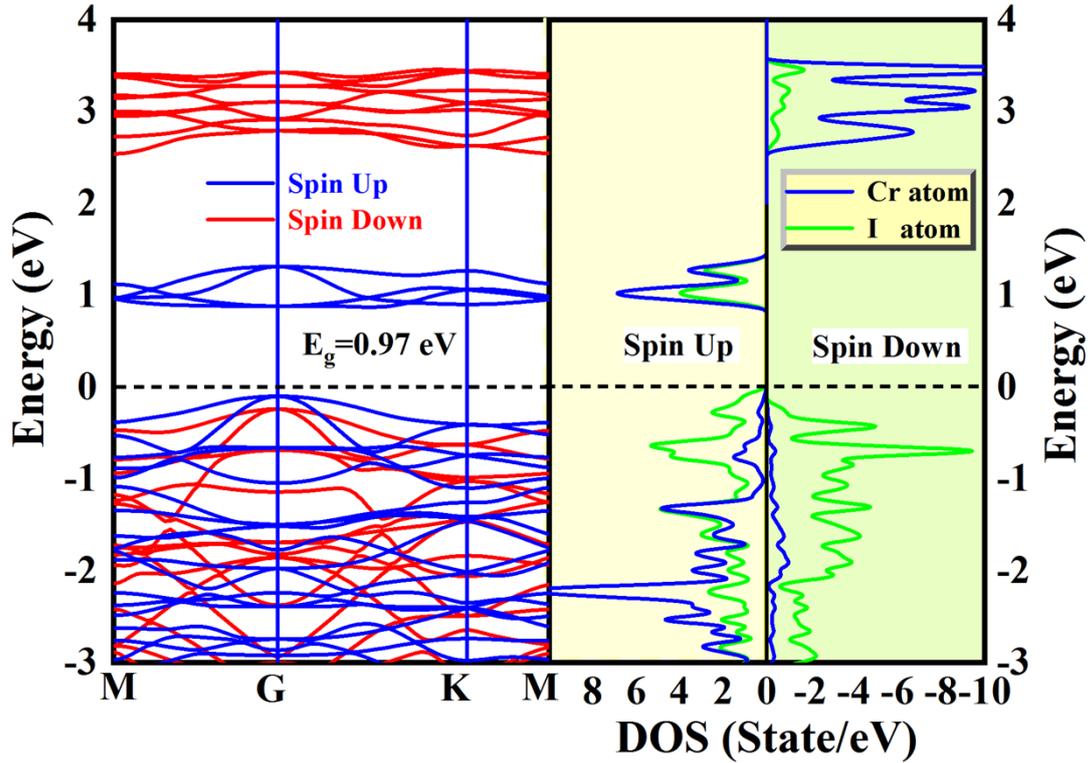
FIG. S1 The spin-polarized band structure and the density of state (DOS) of the monolayer CrI_3 obtained with PBE+U calculations. The blue and red curves denote the spin-up and spin-down bands (left panel), respectively; blue and green lines denote the Cr and I atoms (right panel), respectively.
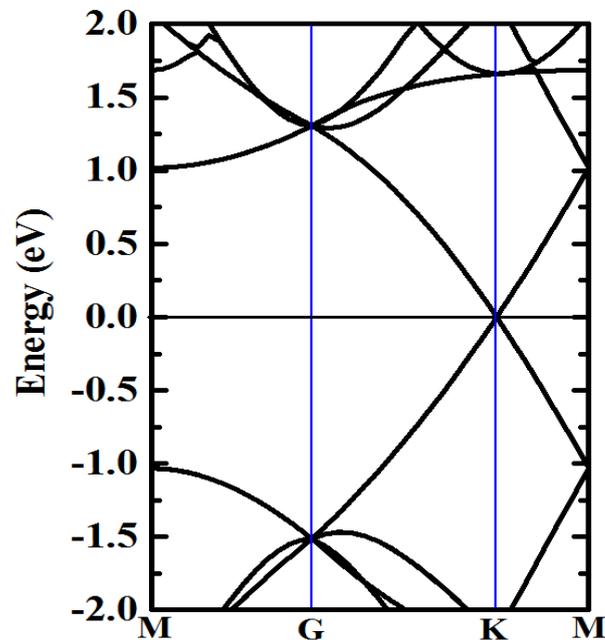

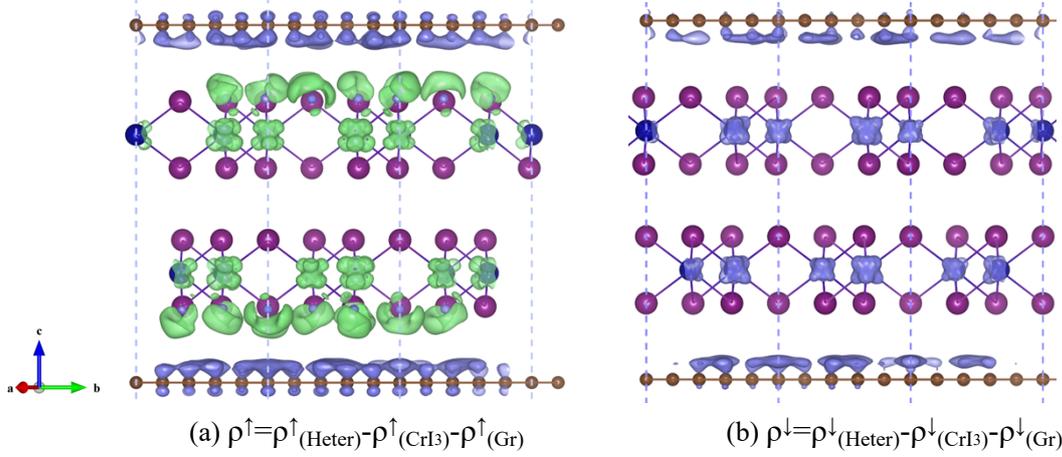**FIG. S2** The band structure of the graphene monolayer obtained with PBE+U calculations.

(a) $\rho^{\uparrow}=\rho^{\uparrow}_{(Heter)}-\rho^{\uparrow}_{(CrI3)}-\rho^{\uparrow}_{(Gr)}$ (b) $\rho^{\downarrow}=\rho^{\downarrow}_{(Heter)}-\rho^{\downarrow}_{(CrI3)}-\rho^{\downarrow}_{(Gr)}$

FIG. S3. (a) Spin-up density difference and (b) spin-down density difference $\rho=\rho_{(Heter)}-\rho_{(CrI3)}-\rho_{(Gr)}$ of Gr|2ML-CrI$_3$|Gr heterostructure from side-view (Isosurface value: 0.0015 e/Å^3) . Green and blue colors denote the accumulation and depletion of density regions, respectively.

Note:

(i) The charge transferred from the spin-up states is more than that from the spin-down states for Gr layers, resulting in the negative magnetic moment on C atoms; (ii) all the charges transferred from Gr layers are filled in the spin-up states of CrI$_3$ layers, indicating that the band gap and thus the spin-dependent tunneling barrier height will be changed to influence the transport properties; (iii) charge transfers from the spin-down states (blue colors in Fig.S3b) to the spin-up states in Cr atoms (green colors in Fig.S3a) will enhance the local magnetic moment of Cr atoms.
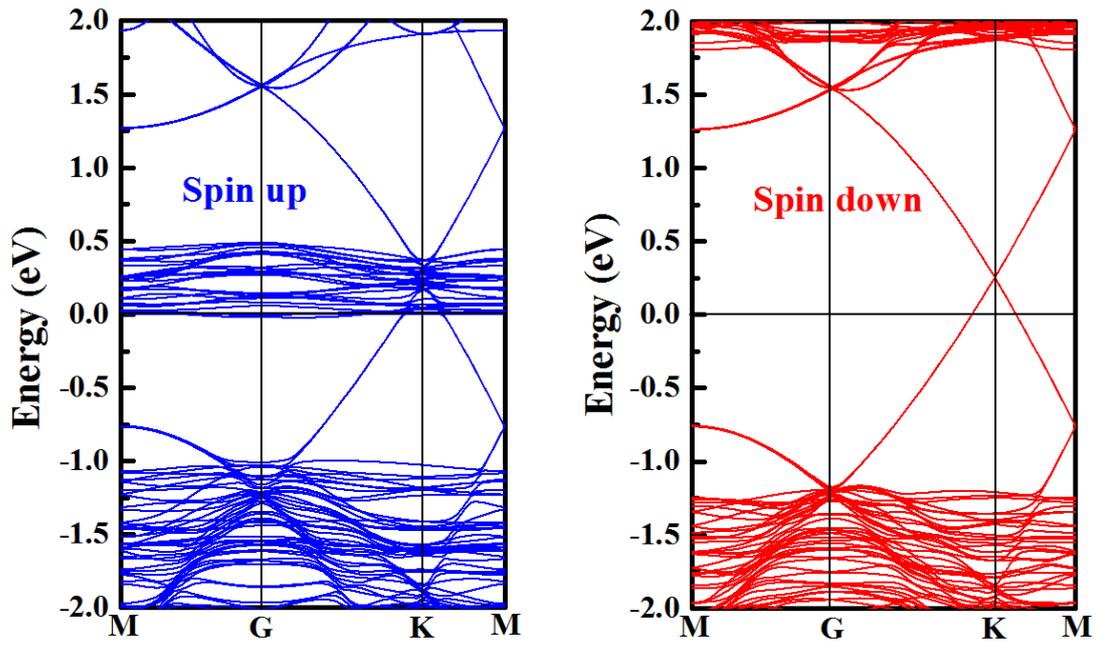
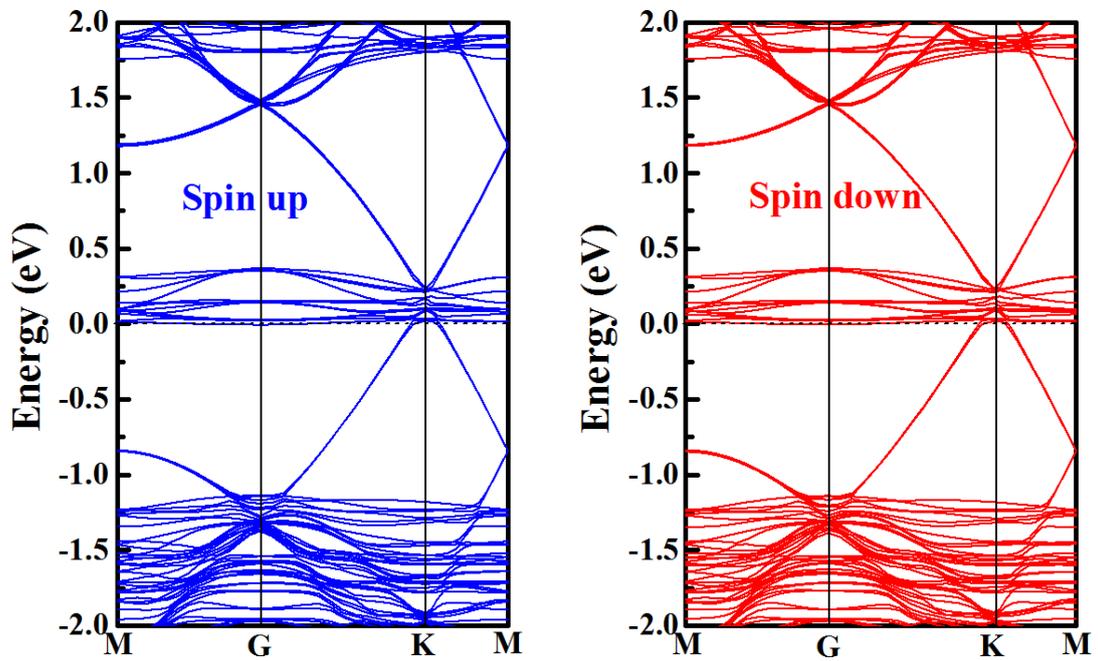**FIG. S4.** Band structures of Gr|2ML-CrI$_3$(AB')|Gr heterostructure with inter-layer ferromagetic (FM) ordering between CrI$_3$ layers.

FIG. S5. Band structures of Gr|2ML-CrI$_3$(AB')|Gr heterostructure with inter-layer antiferromagetic (AFM) ordering between CrI$_3$ layers.